

Theoretical analysis of wandering of commercial vehicles on damaged road surfaces

N. NAGAI and K. KOIKE, Department of Mechanical and Engineering, Tokyo University of Agriculture and Technology, Japan

This paper shows the theoretical analysis of the wandering phenomenon using characteristic equation of the vehicle body. At first the equations of the vehicle motions on the dented wheel tracks on damaged roads are introduced and linearized to get a Laplace - transformed characteristic equation, considering the interaction between the inherent vehicle dynamics and the dented track profiles. By this fourth order equation, the vehicle body fluctuations on the dented tracks are theoretically discussed and verified by computer simulation. It is found that the vehicle body fluctuations on dented tracks are much influenced by forward velocity, wheel track depth, and vehicle parameters.

1. INTRODUCTION

Highway goods transportation by heavy commercial vehicles became to play the most important role for a long distance transportation in Japan. Drivers are sometimes forced to drive the vehicles all day long or even during all night at high speeds so that higher vehicle safety and stability became required than before. Moreover because of increasing number of the heavy commercial vehicles, the damaged and dented road surfaces are often found along the wheel tracks of the heavy vehicles.

When running on such damaged roads, "wandering" phenomenon of the vehicle often occurs and the vehicle stability sometimes becomes to be unstable and dangerous. Nevertheless the fundamental characteristic of the wandering is not clear from the viewpoint of vehicle dynamics, though there have been few experimental researches or computer simulation works.

This paper shows the theoretical analysis of the wandering phenomenon using characteristic equation of the vehicle body. At first the equations of the vehicle motions on the dented wheel tracks on damaged roads are introduced and linearized to get a Laplace - transformed characteristic equation. The stability of vehicles running on the dented tracks can be discussed theoretically by analyzing this equation. Then computer simulation is carried out to verify the theoretical analysis. By the theoretical and numerical analyses, it is clearly explained that the vehicle body fluctuation on dented tracks is influenced by forward velocity, wheel track depth, tire characteristics and vehicle sizes.

Nomenclature

- C_{pi} : cornering power of i - th tire
- C_{si} : camber stiffness of i - th tire
- d_f : tread of front axle
- d_r : tread of rear axle

- F_{ij} : lateral force acting on i - th, j - th tire
- h : depth of a dented track
- I : yaw moment of inertia
- l : wheel base
- l_f : distance between front axle & C.G.
- l_r : distance between rear axle & C.G.
- m : mass of vehicle body
- m_{fg} : weight on front axle
- m_{rg} : weight on rear axle
- V : forward velocity
- W : width of a dented track
- W_b : distance between dented track center lines
- W_c : $W_c = W_b - W$
- y : lateral position of C.G.
- y_{ij} : lateral position of i - th, j - th tire
- β : side slip angle of C.G.
- β_i : side slip angle of i - th tire
- γ : yaw rate of vehicle body
- θ : yaw angle of vehicle body
- ψ_{ij} : camber angle of i - th, j - th tire
- i : f = front: r = rear
- j : 1 = right: 2 = left

2. THEORETICAL MODEL

2.1. Description of dented tracks

Fig.1 shows the geometrical relationship between the dented wheel tracks and the vehicle tires when the vehicle runs along x -axis. The upper figure shows the size of the vehicle and the location of four tires on $x - y$ coordinates, while the lower one shows the cross section of dented wheel tracks on $y - z$ coordinates.

In the following analysis, the cross sectional shape of a wheel track is assumed to be a cosine curve in the lateral direction, and the shape is the same in the longitudinal direction. The track shape of the right hand side is expressed by

$$z_{i1} = \frac{h}{2} \left\{ \cos \frac{2\pi}{W} \left(y_{i1} + \frac{W_c}{2} \right) - 1 \right\} \quad (1)$$

when

$$-W - \frac{W_c}{2} \leq y_{i1} \leq -\frac{W_c}{2}$$

where the suffix $i(=f \text{ or } r)$ denotes the front or rear tire. The track shape of the left hand side is also expressed by

$$z_{i2} = \frac{h}{2} \left\{ \cos \frac{2\pi}{W} \left(y_{i2} - \frac{W_c}{2} \right) - 1 \right\} \quad (2)$$

when

$$\frac{W_c}{2} \leq y_{i2} \leq W + \frac{W_c}{2}$$

As it is supposed that the track may be dented mainly by the rear tires, the lateral distance between both tracks is nearly equal to the tread of rear wheel axle.

2.2. Description of tire forces

Lateral forces acting on each tire considered in this paper are divided into the following forces;

- (1) cornering force proportional to the side slip angle of tire,
- (2) camber thrust proportional to the camber angle against the road surface,
- (3) tangential component of vertical load acting on tire.

Fig.2 shows the cross sectional profile of a tire on dented road where the camber thrust and the tangential component of the vertical load are expressed. The sum of the lateral forces on each tire is therefore expressed by

$$F_{ij} = -C_{pi}\beta_i + \left(\frac{m_i g}{2} - C_{si} \right) \psi_{ij} \quad (3)$$

where C_{pi} , C_{si} and $m_i g/2$ are the cornering power, the camber thrust stiffness and the vertical load of each tire respectively. The suffix $i(=f \text{ or } r)$ denotes the front or rear tire, and the suffix $j(=1 \text{ or } 2)$ denotes the right or left tire.

This expression is derived by linearizing the forces on the assumption that the tire side slip angle β_i and the camber angle ψ_{ij} are relatively small in this analysis.

2.3. Equation of vehicle motion

As this paper focuses on an analytical method to study the interaction between inherent vehicle dynamics and the dented wheel track geometry, a mathematical model of the vehicle is simply expressed by the lateral and yaw motions of the vehicle body as follows. The roll motion and its influence on tires are neglected in this analysis.

$$mV(\dot{\beta} + \gamma) = F_{f1} + F_{f2} + F_{r1} + F_{r2} \quad (4)$$

$$I\dot{\gamma} = \ell_f(F_{f1} + F_{f2}) - \ell_r(F_{r1} + F_{r2}) \quad (5)$$

where the lateral forces are expressed by

$$F_{f1} = -C_{pf}\beta_f + \left(\frac{m_f g}{2} - C_{sf} \right) \psi_{f1} \quad (6)$$

$$F_{f2} = -C_{pf}\beta_f + \left(\frac{m_f g}{2} - C_{sf} \right) \psi_{f2} \quad (7)$$

$$F_{r1} = -C_{pr}\beta_r + \left(\frac{m_r g}{2} - C_{sr} \right) \psi_{r1} \quad (8)$$

$$F_{r2} = -C_{pr}\beta_r + \left(\frac{m_r g}{2} - C_{sr} \right) \psi_{r2} \quad (9)$$

The side slip angles of the front and rear tires are generally expressed by

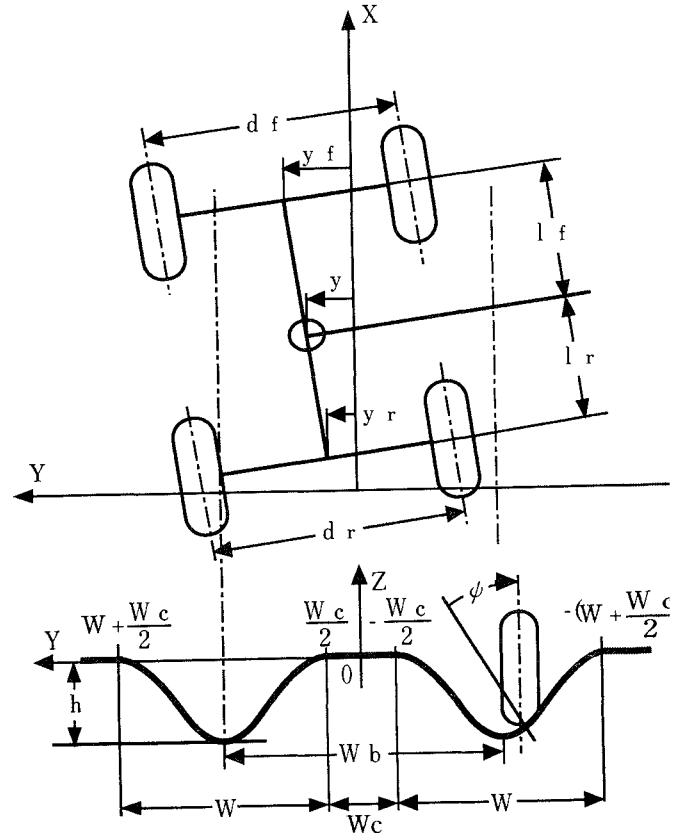


Fig.1 A vehicle model on dented wheel tracks

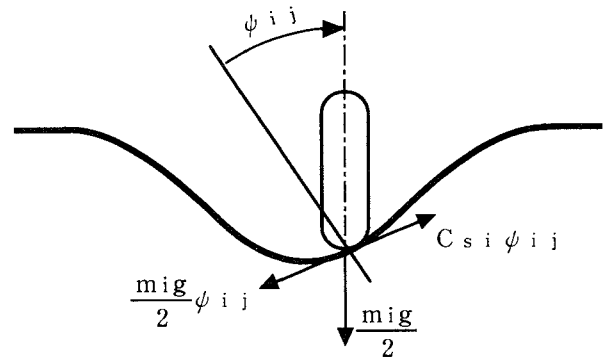


Fig.2 Tire forces and camber angle

$$\beta_f = \beta + \frac{\ell_f}{V}\gamma - \delta_f \quad (10)$$

$$\beta_r = \beta - \frac{\ell_r}{V}\gamma \quad (11)$$

Substituting eqs.(6) ~ (11) into eqs.(4) and (5), the equations of motions concerning the side slip angle β and the yaw rate γ of the vehicle body are reduced to

$$\begin{aligned} & mV\dot{\beta} + 2(C_{pf} + C_{pr})\beta + \{mV + \frac{2}{V}(\ell_f C_{pf} - \ell_r C_{pr})\}\gamma \\ & = 2C_{pf}\delta_f \\ & + (\frac{m_f g}{2} - C_{sf})(\psi_{f1} + \psi_{f2}) \\ & + (\frac{m_r g}{2} - C_{sr})(\psi_{r1} + \psi_{r2}) \quad (12) \\ & 2(\ell_f C_{pf} - \ell_r C_{pr})\beta + I\dot{\gamma} + \frac{2(\ell_f^2 C_{pf} + \ell_r^2 C_{pr})}{V}\gamma \\ & = 2C_{pf}\ell_f\delta_f \\ & + \ell_f(\frac{m_f g}{2} - C_{sf})(\psi_{f1} + \psi_{f2}) \\ & - \ell_r(\frac{m_r g}{2} - C_{sr})(\psi_{r1} + \psi_{r2}) \quad (13) \end{aligned}$$

These equations become very familiar in a case of simple analysis of stability and handling performances on even road surfaces when the camber angles are neglected, that is, $\psi_{f1} + \psi_{f2} = \psi_{r1} + \psi_{r2} = 0$. If these camber angles are assumed to be only the inputs to these equations, this mathematical model is the second order dynamical system.

2.4. Interaction between vehicles and tracks

The camber angles in eqs.(12),(13) are greatly related with the displacement of tires on the dented tracks so that they must be considered as the variables of this dynamical system. This paper therefore analyzes the interaction between the vehicle body dynamics and the camber angle variations due to the dented track unevenness.

In this analysis, there is no input by a driver, that is, the front wheel steer angle δ_f is assumed to be zero. And all equations are linearized, assuming that the vehicle body does not fluctuate so much around the equilibrium position on the dented tracks. The lateral position of each tire on the $x - y$ coordinates shown in Fig.1 is calculated by the following geometrical expressions;

$$y_{f1} = y + \ell_f\theta - d_f/2 \quad (14)$$

$$y_{f2} = y + \ell_f\theta + d_f/2 \quad (15)$$

$$y_{r1} = y - \ell_r\theta - d_r/2 \quad (16)$$

$$y_{r2} = y - \ell_r\theta + d_r/2 \quad (17)$$

where the yaw angle θ and the lateral position y of the vehicle body center of gravity are calculated by the following integral operations.

$$\theta = \theta_0 + \int_0^t \gamma dt \quad (18)$$

$$\begin{aligned} y & = y_0 + \int_0^t V \sin(\beta + \theta) dt \\ & \simeq y_0 + \int_0^t V(\beta + \theta) dt \quad (19) \end{aligned}$$

As the roll motion of the vehicle body is neglected in this paper, the camber angle shown in Fig.2 is equal to the derivative of the shape of the dented track surface.

right:

$$\psi_{i1} = -\frac{\partial z_{i1}}{\partial y} = \frac{\pi h}{W} \sin \frac{2\pi}{W}(y_{i1} + \frac{W_c}{2}) \quad (20)$$

left:

$$\psi_{i2} = -\frac{\partial z_{i2}}{\partial y} = \frac{\pi h}{W} \sin \frac{2\pi}{W}(y_{i2} - \frac{W_c}{2}) \quad (21)$$

where the suffix $i = (f \text{ or } r)$ denotes the front or rear tire respectively.

The sum of these right and left camber angles $\psi_{f1} + \psi_{f2}$, appearing in eqs.(12) and (13), is calculated and reformed to be a function of the lateral position y and the yaw angle θ of the vehicle body as follows.

$$\begin{aligned} & \psi_{f1} + \psi_{f2} \\ & = \frac{\pi h}{W} \left\{ \sin \frac{2\pi}{W}(y_{f1} + \frac{W_c}{2}) + \sin \frac{2\pi}{W}(y_{f2} - \frac{W_c}{2}) \right\} \\ & = \frac{\pi h}{W} \left\{ \sin \frac{2\pi}{W}(y + \ell_f\theta - \frac{d_f}{2} + \frac{W_c}{2}) \right. \\ & \quad \left. + \sin \frac{2\pi}{W}(y + \ell_f\theta + \frac{d_f}{2} - \frac{W_c}{2}) \right\} \\ & = 2\frac{\pi h}{W} \sin \frac{2\pi}{W}(y + \ell_f\theta) \cos \frac{2\pi}{W}(\frac{d_f}{2} - \frac{W_c}{2}) \\ & \simeq \frac{4\pi^2 h}{W^2} \cos \left\{ \frac{\pi}{W}(d_f - W_c) \right\} (y + \ell_f\theta) \quad (22) \end{aligned}$$

This is simply expressed by

$$\psi_{f1} + \psi_{f2} = -A_f(y + \ell_f\theta) \quad (23)$$

where

$$A_f = \frac{4\pi^2 h}{W^2} \cos \frac{\pi}{W} \{d_f - (W_c + W)\} \quad (24)$$

In the same way, the sum of the right and left camber angles $\psi_{r1} + \psi_{r2}$, appearing in eqs.(12) and (13), is simply expressed by

$$\psi_{r1} + \psi_{r2} = -A_r(y + \ell_r\theta) \quad (25)$$

where

$$A_r = \frac{4\pi^2 h}{W^2} \cos \frac{\pi}{W} \{d_r - (W_c + W)\} \quad (26)$$

Substituting eqs.(18),(19) into eqs.(23),(25), the sums of the cabmer angles in front and rear axles are respectively written by

$$\begin{aligned} \psi_{f1} + \psi_{f2} \\ = -A_f \left(\int_0^t V \beta dt + \int_0^t \int_0^t V \gamma dt dt + \int_0^t \ell_f \gamma dt \right) \end{aligned} \quad (27)$$

$$\begin{aligned} \psi_{r1} + \psi_{r2} \\ = -A_r \left(\int_0^t V \beta dt + \int_0^t \int_0^t V \gamma dt dt - \int_0^t \ell_r \gamma dt \right) \end{aligned} \quad (28)$$

when $y_0 = \theta_0 = 0$ in eqs.(18),(19).

As a result, the vehicle body motion on dented wheel tracks is therefore governed by eqs.(12),(13),(27) and (28).

3. CHARACTERISTIC EQUATION

Substituting eqs.(27),(28) into eqs.(12),(13) and using Laplace transformation, characteristic equation of the vehicle running along the dented wheel tracks is described by the following fourth order equation.

$$S^4 + b_1 S^3 + b_2 S^2 + b_3 S + b_4 = 0 \quad (29)$$

where

$$b_1 = \frac{2m(\ell_f^2 C_{pf} + \ell_r^2 C_{pr}) + 2I(C_{pf} + C_{pr})}{mIV} \quad (30)$$

$$\begin{aligned} b_2 = \frac{A_f C_f \ell_f^2 + A_r C_r \ell_r^2 - 2(\ell_f C_{pf} - \ell_r C_{pr})}{I} \\ + \frac{A_f C_f + A_r C_r}{m} + \frac{4}{mIV^2} C_{pf} C_{pr} l^2 \end{aligned} \quad (31)$$

$$b_3 = \frac{2(C_{pf} A_r C_r + C_{pr} A_f C_f) l^2}{mIV} \quad (32)$$

$$b_4 = \frac{-2I(C_{pf} A_r C_r - C_{pr} A_f C_f) + A_f A_r C_f C_r l^2}{mI} \quad (33)$$

$$C_f = \frac{m_f g}{2} - C_{sf} \quad (34)$$

$$C_r = \frac{m_r g}{2} - C_{sr} \quad (35)$$

If the road surface is even without the influence of dented tracks, the coefficients in eqs.(24),(26) and eqs.(32),(33) are zero.

$$h = 0 \quad \Rightarrow \quad A_f = A_r = 0 \quad (36)$$

$$\Rightarrow \quad b_3 = b_4 = 0 \quad (37)$$

Therefore the characteristic equation of the vehicle motion on even surface becomes to be a familiar form as follows.

$$S^2(S^2 + b_{01}S + b_{02}) = 0 \quad (38)$$

where

$$\begin{aligned} b_{01} &= b_1 \\ &= \frac{2m(\ell_f^2 C_{pf} + \ell_r^2 C_{pr}) + 2I(C_{pf} + C_{pr})}{mIV} \end{aligned} \quad (39)$$

$$b_{02} = \frac{-2(\ell_f C_{pf} - \ell_r C_{pr})}{I} + \frac{4}{mIV^2} C_{pf} C_{pr} l^2 \quad (40)$$

Stability of the vehicle on even road is usually evaluated by the coefficients of this equation. The understeer (US) or oversteer (OS) characteristics are defined by

$$\text{US when } \ell_r C_{pr} - \ell_f C_{pf} > 0$$

$$\text{OS when } \ell_r C_{pr} - \ell_f C_{pf} < 0$$

by which handling and stability performances on even road surfaces are often evaluated.

Table 1 Baseline parameters

m	1.43 x 10 ⁴ kg	I	1.76 x 10 ⁵ kgm ²
d_f	2.0 m	d_r	1.8 m
ℓ_f	4.0 m	ℓ_r	2.6 m
m_{fg}	5.5 x 10 ⁴ N	m_{rg}	8.8 x 10 ⁴ N
C_{pf}	1.4 x 10 ⁵ N/rad	C_{pr}	2.8 x 10 ⁵ N/rad
C_{sf}	2.8 x 10 ³ N/rad	C_{sr}	5.6 x 10 ³ N/rad
W	1.2 m	W_b	1.8 m

4. ANALYSIS OF CHARACTERISTIC ROOTS

Table 1 shows the baseline parameters of a commercial vehicle and dented tracks in this paper. Stability of the vehicle motion on the dented tracks can be discussed by the locations of characteristic roots which are the solutions of the characteristic equation (29). As it is the fourth order equation, the roots are mostly divided into two pairs of complex number, which physically represent the two degree-of-freedom motions combined by the yaw and lateral motions of the vehicle body. Two pairs of roots are separately depicted in a complex plane for the convenience of description.

Fig.3 shows the characteristic roots of eq.(29) in the complex plane, on which the depth of the dented tracks h has a large influence at each forward velocity. When the depth h is zero, the roots depicted in the lower part converge to zero of this complex plane. This means that the roots appearing in the lower part directly represent

the original roots subject to the dented tracks. On the other hand, the roots depicted in the upper part converge to those which are the solutions of the characteristic equation (38) on even road surfaces. Therefore, the roots in the upper part correspond to the original vehicle dynamic stability. Nevertheless it is obvious that these roots are greatly interacted by each other and influenced by the parameters of the vehicles and tracks.

According to the results in Fig.3, it is clearly found that stability decreases at high speeds because all roots move in the direction to the imaginary axis when the forward velocity increases. And it is also found that the damping coefficients become smaller when the dented tracks become deeper. Therefore the vehicle is liable to fluctuate by a certain disturbance when running at high speeds on deeply dented tracks. This theoretically obtained tendency has a good agreement with driving situations we often face.

In order to make clear these influences on dynamic characteristics, the damping coefficients and damped natural frequencies of the vehicle motion corresponding to two pairs of the characteristic roots are calculated and depicted in Fig.4 and Fig.5.

Fig.4 shows the results of the natural frequencies and the damping coefficients versus the forward velocity when the track depth is 0.05 m, comparing with those when the road surface is flat. There are two pairs of them, one of which corresponds to the inherent characteristic root and the other is generated by the track-vehicle interaction. Whether the vehicle body keeps on

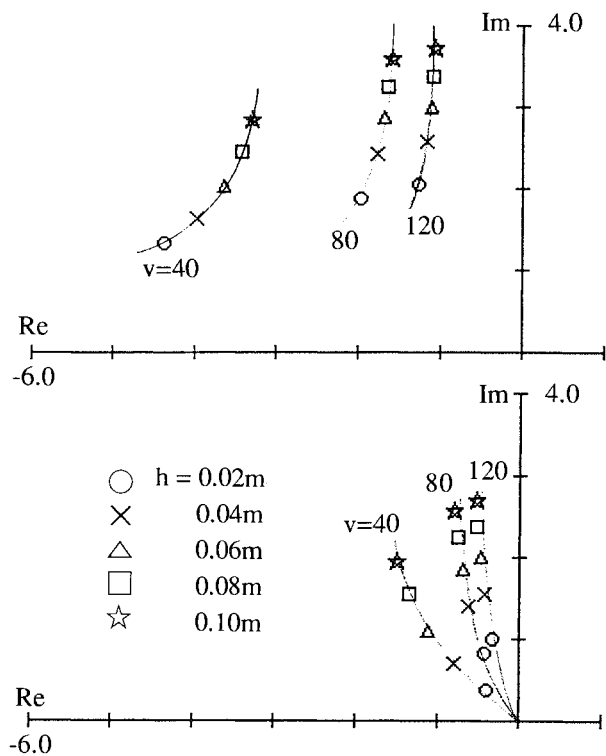


Fig.3 Characteristic roots influenced by forward velocity V and track depth h

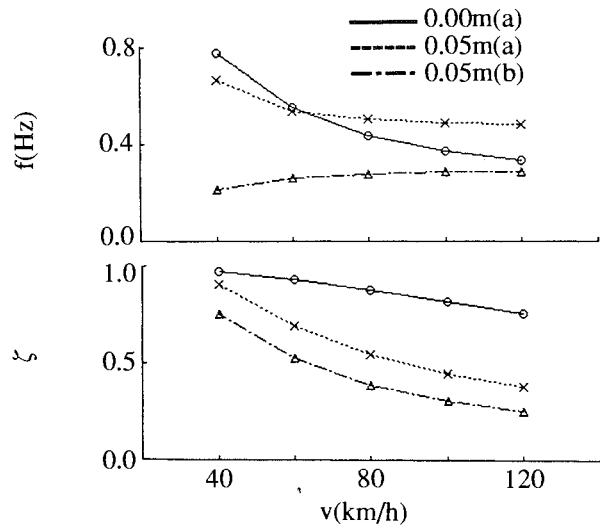


Fig.4 Influence of forward velocity V on the frequency and damping of vehicle body fluctuation

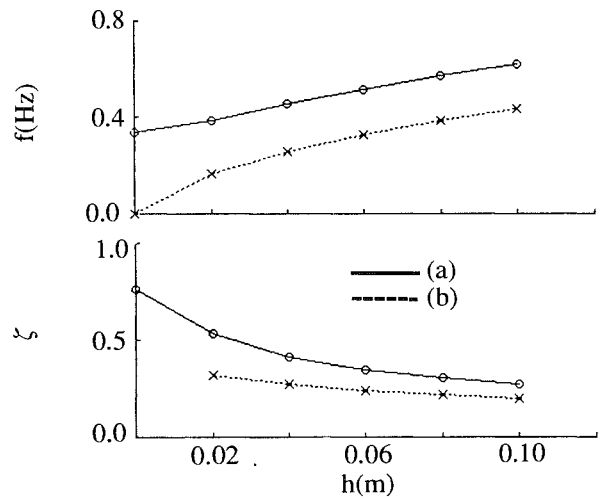


Fig.5 Influence of track depth h on the frequency and damping of vehicle body fluctuation

fluctuating or not is evaluated generally by the value of damping coefficient ζ . According to Fig.4, the damping coefficients ζ decrease approximately in inverse proportion to the forward velocity. Therefore it is theoretically concluded that the vehicle body is liable to fluctuate at high speeds.

Fig.5 shows the natural frequencies and the damping coefficients versus the track depth when the vehicle runs at 120 km/h. Fig.5 indicates that the damping coefficients decrease similarly as shown in Fig.4. Fig.5 also indicates that both natural frequencies become larger when the track depth becomes deeper.

From these results, it is theoretically concluded that the vehicle body is liable to fluctuate by a certain disturbance when running fast on deeply dented tracks, and that the fluctuation frequency becomes larger at higher speeds on deeper tracks, and therefore it might be difficult for a driver to operate the vehicle in such dangerous situations.

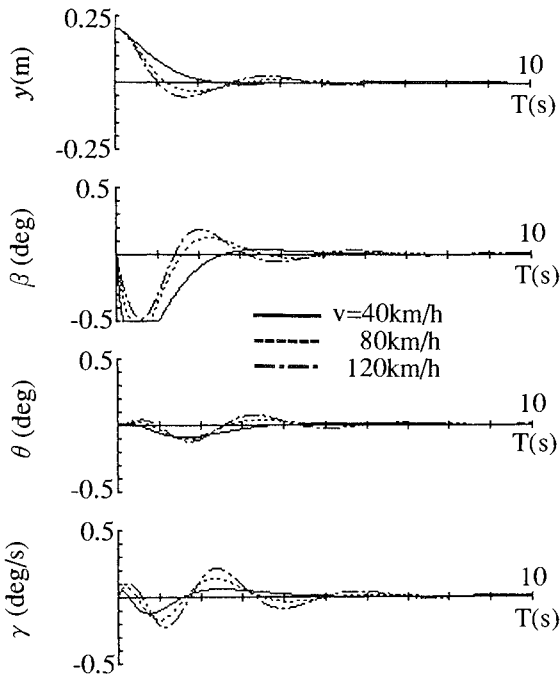


Fig.6 Influence of forward velocity V on the transient responses when $h = 0.05$ m

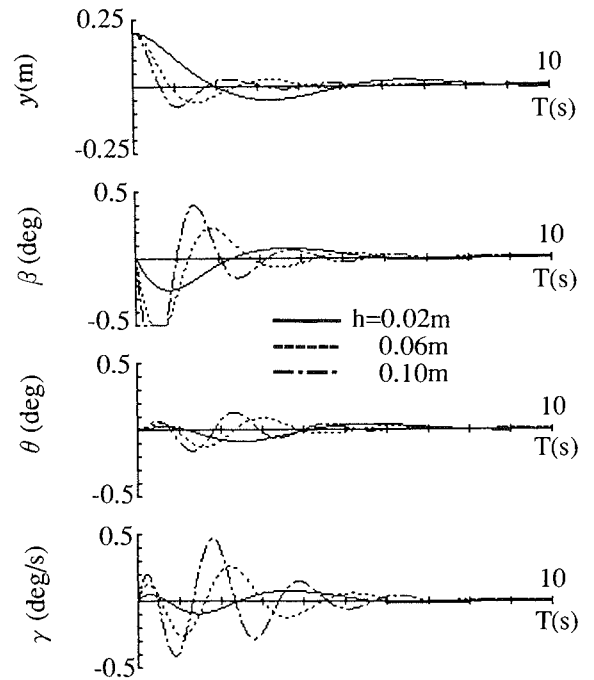


Fig.7 Influence of track depth h on the transient responses when $V = 120$ km/h

5. TRANSIENT RESPONSE

In order to verify these theoretical results, a computer simulation is carried out and compared with above results. The computer simulation shows the transient responses of the vehicle body which is at first displaced from the equilibrium line as the following initial conditions.

$$\begin{aligned}
 y_0 &= 0.20 \text{ m} & , & & \theta_0 &= 0 \text{ rad} \\
 \beta_0 &= 0 \text{ rad} & , & & \gamma_0 &= 0 \text{ rad/s}
 \end{aligned}$$

Fig.6 shows the influences of the forward velocity V on the transient responses of the vehicle body when the track depth h is 0.05 m. These responses clearly indicate that the forward velocity has a great influence on the fluctuation of the lateral displacement and the yaw angle of the vehicle body. This influence is able to be explained by the theoretical results of the damping characteristics shown in Fig.4 where the damping coefficient ζ decreases approximately in inverse proportion to the forward velocity.

Fig.7 shows the influences of the track depth h on the transient responses of the vehicle body running at 120 km/h for ten seconds. These results show a tendency that the responses fluctuate for a longer period when the track depth h becomes larger. Moreover the same results about the natural frequency and damping characteristics are able to be recognized as those shown in Fig.5 in the previous section. The frequency of fluctuation changes approximately from 0.2 to 0.5 Hz and

the damping coefficient becomes less than a half approximately when the track depth h increases from 0.02 to 0.10 m.

6. PARAMETRIC STUDY

The stability of the vehicle body is much influenced by the vehicle parameters, such as, the tire characteristics, the center of gravity location and the tread of axles and others. This section discusses these influences on the yaw rate response by changing these parameters. The baseline parameters in the following calculations are given in the Table 1, and the track depth is 0.05 m and the forward velocity is 120 km/h. The initial conditions of these analyses are the same as above.

6.1. Influence of cornering power

Fig.8 shows the influence of the cornering powers of the front and rear tires on the transient responses of the yaw rate. Fig.8(a) shows the case where both front and rear values, C_{pf} and C_{pr} , are changed simultaneously, while Fig.8(b) and Fig.8(c) show the cases where the front or rear value, C_{pf} or C_{pr} , is changed respectively. From the result in Fig.8(a), the damping of the transient response becomes lower when the two values decrease from the baseline value, while the frequency of fluctuation is almost the same. From the results in Fig.8(b) and Fig.8(c), the fluctuation becomes larger when the front cornering power decreases or the rear one increases. Therefore it is important to notify that the deterioration of the front tire cornering power has a bad influence on the fluctuation.

6.2. Influence of camber thrust

Fig.9 shows the influence of the camber thrust stiffness of the front and rear tires on the transient responses of the yaw rate. Fig.9(a) shows the case where both front and rear values, C_{sf} and C_{sr} , are changed simultaneously, while Fig.9(b) and Fig.9(c) show the cases where the front or rear value, C_{sf} or C_{sr} , is changed respectively. The results in Fig.9 show nearly the same tendencies as those in Fig.8. From the results in Fig.9(b) and Fig.9(c), the fluctuation becomes larger when the front camber stiffness decreases or the rear one increases. Therefore it is important to notify that the deterioration of the front tire camber stiffness has a bad influence on the fluctuation.

6.3. Influence of center of gravity

Fig.10 shows the influence of the location of the center of gravity on the transient responses of the yaw rate,

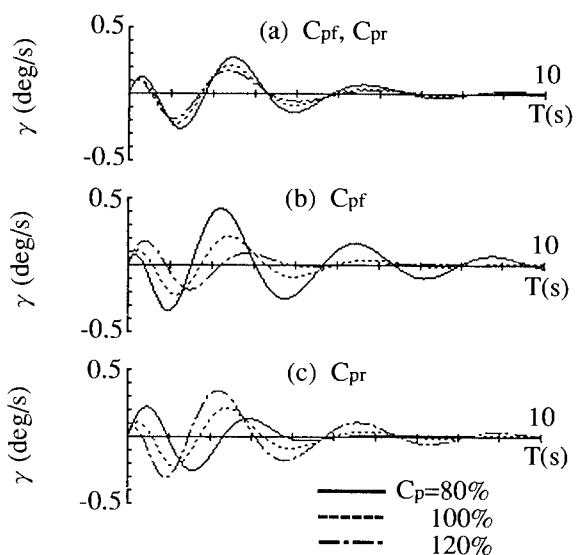


Fig.8 Influence of cornering powers on the yaw rate response when $V = 120 \text{ km/h}$, $h = 0.05 \text{ m}$

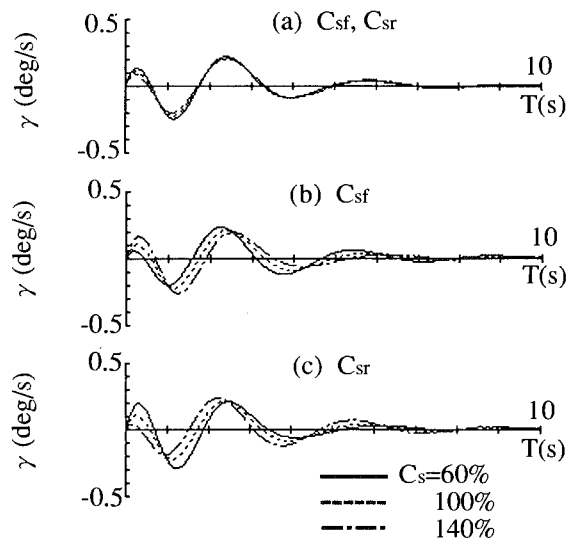


Fig.9 Influence of camber thrust stiffness on the yaw rate response when $V = 120 \text{ km/h}$, $h = 0.05 \text{ m}$

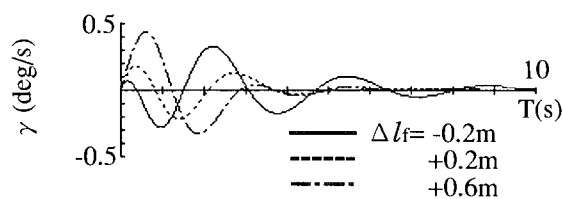


Fig.10 Influence of the center of gravity on the yaw rate response when $V = 120 \text{ km/h}$, $h = 0.05 \text{ m}$

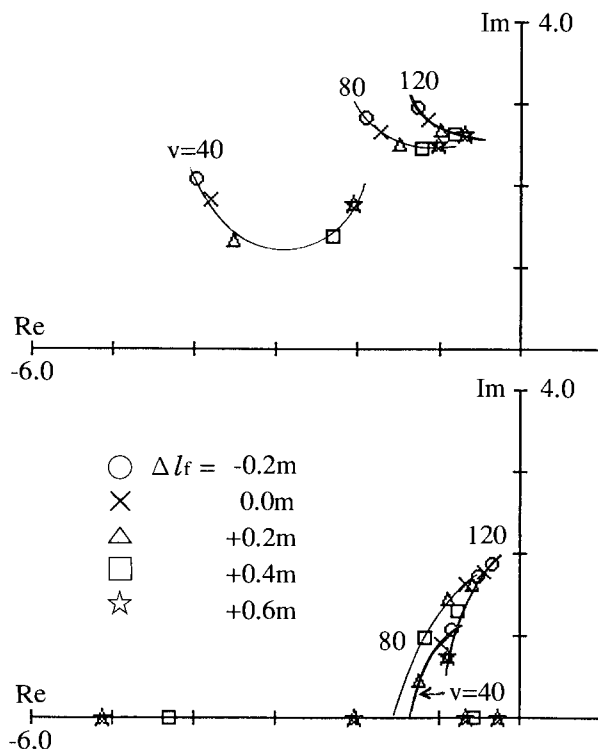


Fig.11 Influence of the center of gravity on characteristic roots when $V = 120 \text{ km/h}$, $h = 0.05 \text{ m}$

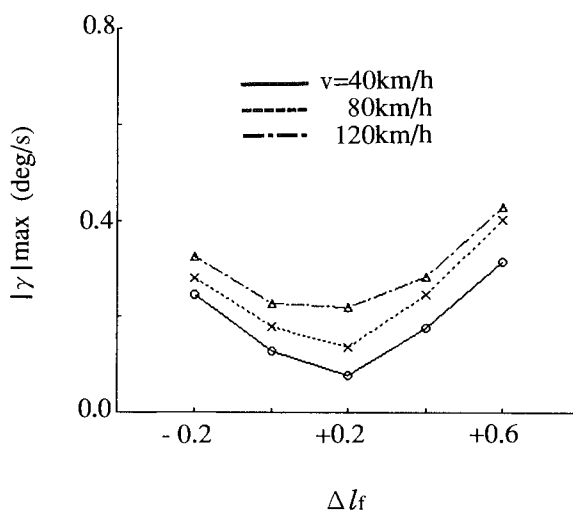


Fig.12 Comparison of the maximum amplitude of the yaw rate response subject to the center of gravity

while Fig.11 shows the influence on the characteristic roots. The influence of the C.G. location appears clearly on the responses. Although the fluctuation is almost suppressed at an appropriate value of l_f , the time history of the transient response changes in different manners when the value l_f increases or decreases.

It may be because the two characteristic roots shown in Fig.11 are located nearly in such a same area that the influence of them appears on the response to the same extent. Moreover it is found that the two damping coefficients have different influences by the value l_f . This means that the damping of the upper root becomes small at large l_f , while the damping of the lower root becomes small at small l_f . As a result, the fluctuation amplitude is very sensitive to the location of C.G. according to the comparison of the maximum amplitudes of yaw rate transient responses shown in Fig.12.

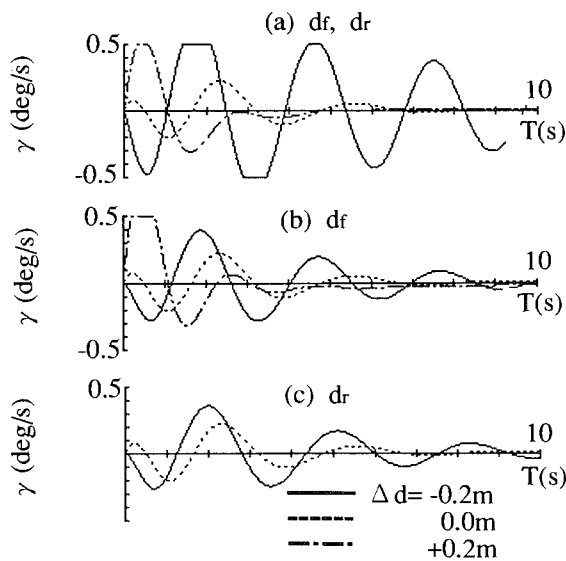


Fig.13 Influence of axle treads on the yaw rate response when $V = 120 \text{ km/h}$, $h = 0.05 \text{ m}$

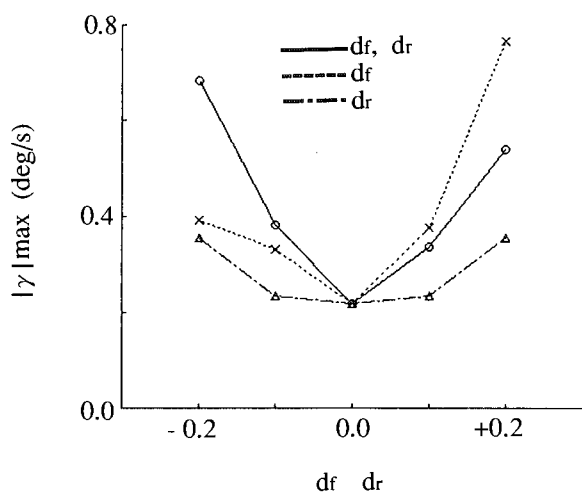


Fig.14 Comparison of the maximum amplitude of the yaw rate response subject to axle treads

6.4. Influence of axle treads

Fig.13 shows the influence of the tread of the front and rear axles on the transient responses of the yaw rate. Fig.13(a) shows the case where both front and rear values, d_f and d_r , are changed simultaneously, while Fig.13(b) and Fig.13(c) show the cases where the front or rear value is changed respectively. In these comparisons there is a large influence of the axle treads on the fluctuation of the yaw rate response. Especially the vehicle body fluctuates very large whenever the treads of front and rear axles become small simultaneously or respectively. As the comparison of the maximum amplitudes of the yaw rate transient responses is shown in Fig.14, the fluctuation amplitude is very sensitive to the axle treads. This result may somehow show one of the reasons why small or medium busses or trucks often face a wandering, vehicle body fluctuation, on the wheel tracks dented by heavy vehicles.

7. CONCLUSIONS

This paper has theoretically analyzed the stability of vehicles running on damaged tracks which are dented by heavy vehicles. For this analysis, the fourth order characteristic equation of vehicle dynamics on the dented tracks has been introduced, based on linearization and Laplace transformation of the equations of motions considering the interaction between vehicle dynamics and track profiles. By using this characteristic equation, fundamental characteristics on the wandering phenomenon are able to be predicted theoretically, which have a good agreement with the results of computer simulation.

From the analyses, it can be theoretically explained that the vehicle body is liable to fluctuate with low damping when running fast on deeply dented tracks, and that the fluctuation frequency becomes larger at higher speeds on deeper tracks, and therefore it might be difficult for a driver to operate the vehicle in such dangerous driving situations. Moreover it is found that the fluctuation of vehicle body on dented tracks are greatly influenced by tire characteristics, the location of center of gravity and the axle treads of vehicles.

REFERENCES

1. T.Nakatsuji et al., Behavior of Vehicles Running on Dented Roads - Analysis of Experimental Characteristics, Preprints of JSAE, Paper No.862128, 1986.
2. K. Nishimura et al., Analysis of Vehicle Behavior on a Wandering Road, Isuzu Technical Review, No.78, pp.70-78, 1987.
3. K.Koike and M.Nagai, Study on a Wandering Phenomenon along the Wheel Tracks on Damaged Road, (1st Report, Stability Analysis by Characteristic Equation), Preprints of JSAE, Paper No.912161, 1991.